

## A NEW DESIGN OF THE SSC BOOSTERS\*

M. A. Furman and L. K. Chen<sup>†</sup>  
 SSC Central Design Group<sup>‡</sup>  
 Lawrence Berkeley Laboratory  
 Berkeley, CA 94720

A new design for the lattices of the SSC's three injectors is presented [1]. The complex is matched so that the SSC filling factor is 94%, and is designed so that there is no transition crossing at any point. The dispersion function is small overall and vanishes in the straight sections. Tracking simulations which include the effect of the space-charge force, sextupoles, synchrotron oscillations and the expected random and systematic dipole magnet errors indicate that the CDR magnet design allows adequate dynamic aperture for all three boosters, and that the space-charge force in the LEB has no significant detrimental effect provided the LEB is tuned properly.

### Introduction

We present new lattice designs for the three SSC boosters meeting the following desirable features [1]: (1) The dispersion function is small and vanishes in the straight sections. (2) There is no transition energy crossing at any point in the injection chain; and (3) Particle tracking including the effects of the space-charge force, sextupole magnets, dipole magnet errors and synchrotron oscillations shows sufficiently large dynamic aperture and sufficiently good beam quality for the proper operation of the SSC.

Tables 1-3 below provide a comparison between the new design and the CDR [2] (a bunch spacing of 4.76 m is assumed for all three injectors and the SSC). The lattices for all three boosters are based on FODO cells with phase advance close to 90°. There is no transition crossing at any point in the chain, as is also the case in the CDR design. The boosters and the SSC are matched so that the harmonic number of each stage is an approximate multiple of the previous one, so that beam transfers can be done efficiently. An example of the loading scenario [3] is shown in Fig. 1 with a resulting filling factor of 94% for the SSC, as opposed to ~85% in the CDR. We have computed the thresholds for single-bunch instabilities and they seem to be easily achievable. (The parameters related to the longitudinal phase space have not yet been studied systematically).

### Overview and Comparison with the CDR

The LEB is the injector that has undergone the largest relative change, with an increase in circumference from 250 m to 343 m and a reduction in superperiodicity from 5 to 2. The reduction of the dispersion in the straight sections was achieved with dispersion suppressors, which were not used in the CDR design. The lattice functions are smoother and smaller than in the CDR; in particular, the maximum value of the dispersion in the arcs has been reduced from 10 m to 0.84 m. Because of the increased circumference, however, the space-charge tune shift at injection

Table 1. LEB Parameters

	CDR	New Lattice
Injection momentum	1.22	1.22 GeV/c
Extraction momentum	8.0	8.45 GeV/c
Circumference	249.6	342.7 m
Harmonic number	52	72
Number of bunches	52	72
Protons per bunch	$1.0 \times 10^{10}$	$1.0 \times 10^{10}$
Circulating current at extraction	99	100 mA
Norm. transv. emittance ( <i>rms</i> )	0.75	0.75 mm-mrad
Longitudinal emittance ( <i>rms</i> )	1.8	1.8 meV-sec
Horizontal tune	4.39	11.84
Vertical tune	4.41	11.78
Transition gamma	10.5	10.3
Natural chromaticities (H, V)	-5.2, -4.9	-15.3, -15.6
Lattice type	FODO	FODO
Superperiodicity	5	2
Maximum beta (arcs)	21.5	11.9 m
Maximum dispersion	10.1	0.84 m
Number of dipoles	30	16 / 64
Dipole length	4.5	0.9 / 1.8 m
Dipole field (max)	1.24	1.37 T
Full good field aperture (H)	80	80 mm
Number of quadrupoles	40	94
Quadrupole length	0.3	0.6 m
Max. quadrupole strength ( <i>B'</i> )	18.4	20.6 T/m
Full good field aperture	80	80 mm
Number of sextupoles	10	64
Number of sextupole families	2	2
Max. sextupole strength ( <i>1B''</i> )	5.6	48.5 T/m
RF frequency at injection	49.5	49.9 MHz
RF frequency at extraction	62.0	63.0 MHz
RF voltage at injection	350	350 kV
Synchronous phase angle	30°	30°
Cycle time	0.1	0.1 sec

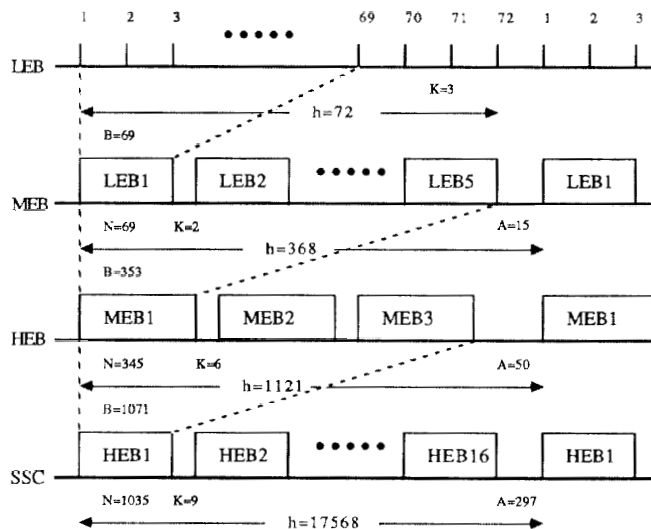


Fig 1: Sample loading scenario. In each train B is the number of buckets, N the number of bunches (filled buckets), h the harmonic number, K and A the kicker and abort gaps, respectively. The resulting SSC filling factor is therefore  $16 \times 3 \times 5 \times 69 / 17568 = 0.94$ .

\* This note is a summary of Ref. [1].

<sup>†</sup> Permanent address: Physics Department, Shenzhen University, People's Republic of China; current address: Texas Accelerator Center, The Woodlands, TX 77380.

<sup>‡</sup> Operated by the Universities Research Association, Inc. for the U. S. Department of Energy.

Table 2. MEB Parameters

	CDR	New Lattice
Injection momentum	8.0	8.45 GeV/c
Extraction momentum	100	100 GeV/c
Circumference	1900.8	1751.6 m
Harmonic number	396	368
Number of bunches	364	345
Protons per bunch	$1.0 \times 10^{10}$	$1.0 \times 10^{10}$
Circulating current	92	95 mA
Norm. transv. emittance ( <i>rms</i> )	0.83	0.83 mm-mrad
Longitudinal emittance ( <i>rms</i> )	1.8	1.8 meV-sec
Horizontal tune	8.41	9.81
Vertical tune	8.41	9.87
Transition gamma	7.2	8.37
Natural chromaticities (H, V)	-9.4, -9.3	-12.5, -12.7
Lattice type	FODO	FODO
Superperiodicity	6	2
Maximum beta (arcs)	67.2	78.1 m
Maximum beta (straights)	67.2	124.0 m
Maximum dispersion	14.2	6.2 m
Number of dipoles	216	128
Dipole length	5.4	9.625 m
Dipole field (max)	1.8	1.7 T
Full good field aperture (H)	80	80 mm
Number of quadrupoles	96	76
Quadrupole length	0.75	1.0 m
Max. quadrupole strength ( <i>B'</i> )	22.8	22.0 T/m
Full good field aperture	80	80 mm
Number of sextupoles	72	56
Number of sextupole families	2	2
Max. sextupole strength ( <i>IB''</i> )	4.4	10.3 T/m
RF frequency	62.5	62.6 MHz
RF voltage	600	600 kV
Synchronous phase angle	30°	30°
Cycle time	4	4 sec

energy has changed from -0.16 to -0.22. This change is potentially detrimental; however, tracking simulations show that this is probably not a serious problem provided the LEB is properly tuned.

The essential modification in the MEB was the addition of dispersion suppressors, which result in a reduction in the maximum dispersion from 14 m to 6 m. The superperiod is now 2 instead of 6 in the CDR.

Good matching requires a shorter circumference for the HEB than in the CDR. In order to achieve this while maintaining 6 relatively long straight sections, the dispersion suppressors had to be eliminated. The dispersion remains small in the arcs and zero in the straight sections thanks to an overall fit.

Fig. 2 shows the lattice functions for the boosters.

### Tracking at Injection Energy

#### Space-Charge Effects

We have done tracking simulations only at injection energy since the space-charge effects are largest at low energy. Our results come from first order, single-particle simulations obtained with the kick code TEAPOT[4] suitably augmented to incorporate the space-charge force[5].

For the purposes of tracking we first adjust the tunes of the lattice to their nominal values (those in Tables 1-3) and the chromaticities to zero. We assume reasonable values for the expected random and systematic errors for the dipole magnets. In general the phase space is quite linear and there is little smear due to nonlinearities. For the LEB, where the space-charge effect is largest, there is a resonance that causes some phase space distortion, as seen in Fig. 3. We believe that this resonance does

Table 3. HEB Parameters

	CDR	New Lattice
Injection momentum	100	100 GeV/c
Extraction momentum	1000	1000 GeV/c
Circumference	6000	5335.8 m
Harmonic number	1250	1121
Number of bunches	1092	1035
Protons per bunch	$1.0 \times 10^{10}$	$1.0 \times 10^{10}$
Circulating current	87	95 mA
Norm. transv. emittance ( <i>rms</i> )	0.91	0.91 mm-mrad
Longitudinal emittance ( <i>rms</i> )	35	35 meV-sec
Horizontal tune	25.415	29.23
Vertical tune	21.415	22.29
Transition gamma	18.7	24.2
Natural chromaticities (H, V)	-66.5, -39.6	-43.0, -32.3
Lattice type	FODO	FODO
Superperiodicity	6	6
Maximum beta (arcs)	117	76.6 m
Maximum beta (straights)	500	267 m
Maximum dispersion	4.2	4.1 m
Number of dipoles	528	384
Dipole length	7.0	9.65 m
Dipole field (max)	5.66	5.66 T
Full good field aperture (H)	26	26 mm
Number of standard quads	150	198
Standard quad length	1.0	1.5 m
Standard quad strength (max)	144.0	133.4 T/m
Full good field aperture	26	26 mm
Number of special quads	36	24
Special quad length	2.0 / 3.0	1.5 / 2.25 m
Special quad strength (max)	144.0	130.1 T/m
Full good field aperture	40	40 mm
Number of sextupoles	138	180
Number of sextupole families	2	2
Sextupole strength (max)	138.0	233.4 T/m
RF frequency	62.5	63.0 MHz
RF voltage	1500	1500 kV
Synchronous phase angle	30°	30°
Cycle time	60	60 sec

not degrade the beam quality significantly, although we have not done a quantitative calculation of the emittance dilution, and we have not assessed its effect during acceleration. It is quite possible that there are other good choices for the operating point; we have not carried out a systematic search.

For the LEB the space-charge tune shifts are  $\Delta\nu_x = -0.21$  and  $\Delta\nu_y = -0.22$ , and for the MEB we obtain  $\Delta\nu_x = -0.060$  and  $\Delta\nu_y = -0.092$ . These values are in good agreement with the "smooth- $\beta$ " estimates from the linear theory[6].

#### Dynamic Aperture

In order to determine the aperture we assume that the vacuum pipe is round and has a radius of 5 cm for the LEB and MEB, and 2 cm for the HEB (the CDR has oval-shape pipes for the LEB, but we assume it round for simplicity in the tracking simulations). By tracking large amplitude particles for 512 turns (with spot-checks of 4,096 turns) with  $\Delta p/p = 3\sigma_p/p$  and with dipole errors we obtain the approximate boundary for stability, *i.e.*, the dynamic aperture. For the LEB the dynamic aperture is essentially equal to the physical aperture. This implies that the nonlinear effects are not significant, and allows for the possibility of redesigning the magnets with smaller bore. For the MEB and HEB the magnet errors are important, resulting in a dynamic aperture smaller by  $\lesssim 20\%$  than the physical aperture; the corresponding "good-field" regions are approximately equal to (indeed, slightly larger than) those specified in the CDR. Of course the dynamic aperture should be reexamined when a more complete and reliable list of errors becomes available.

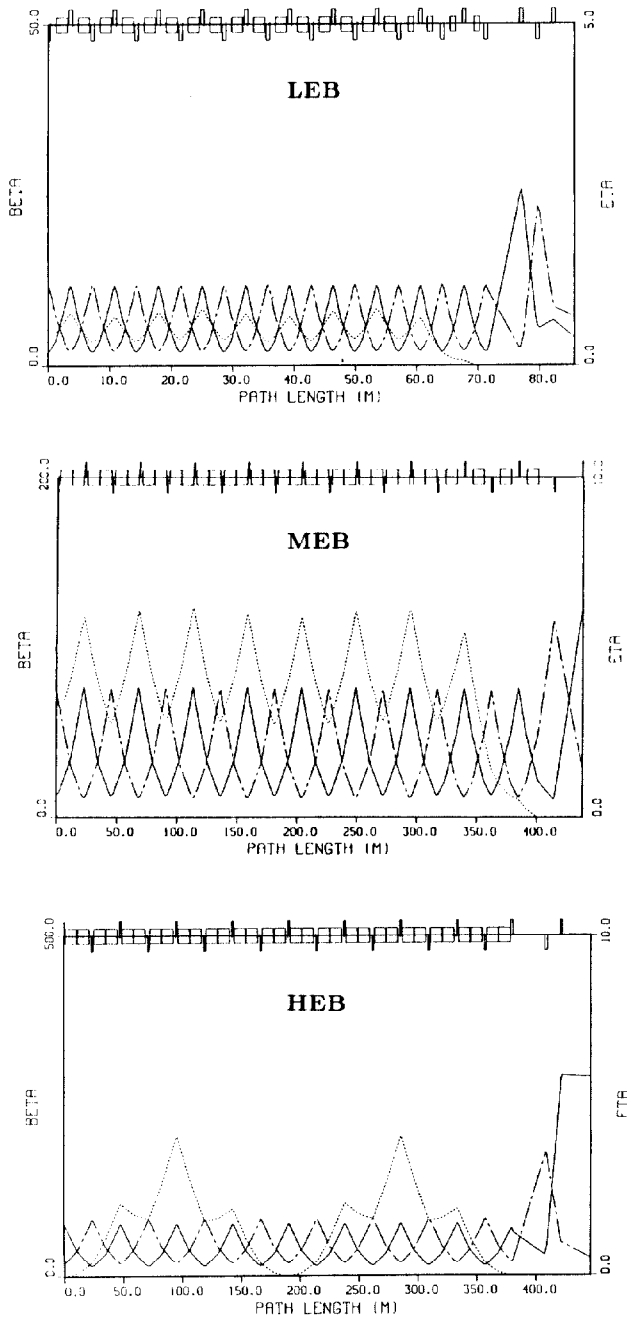


**Fig. 2: Lattice functions for the boosters for one half of a superperiod.** Solid line: horizontal  $\beta$ -function; dot-dash line: vertical  $\beta$ -function; dotted line:  $\eta$ -function. The odd shape of the  $\eta$ -function for the HEB is due to the absence of dispersion suppressors and the  $\sim 90^\circ$  cell structure.

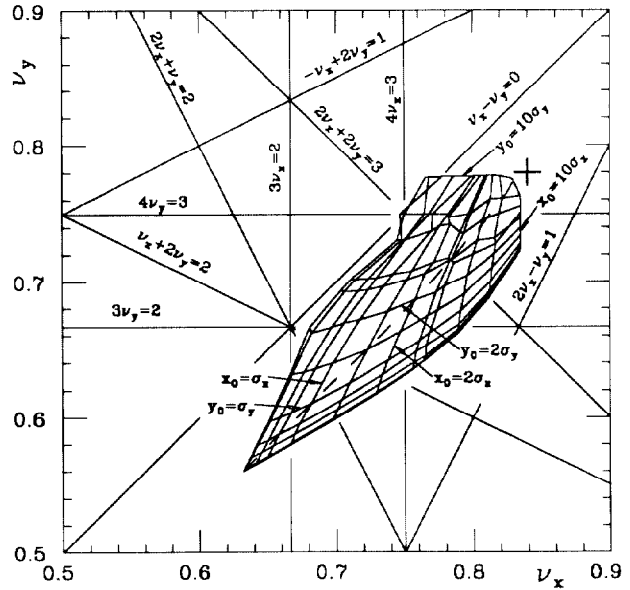


**Fig. 3: Tune distribution of particles in the LEB at injection energy.** The working point is indicated by a heavy cross at  $\nu_x = 11.84$ ,  $\nu_y = 11.78$ . The tip of the “necktie” diagram corresponds to the particles at the center of the bunch, which are tune-shifted due to the space-charge force. The effects of the resonance lines  $\nu_x = 3/4$ ,  $\nu_y = 3/4$  and  $2\nu_x + 2\nu_y = 3$  are apparent in the distortion of the diagram at large amplitudes.

### References

1. L. K. Chen and M. A. Furman, “A Possible New Design of the SSC Boosters,” SSC-164, November 1988.
2. SSC Central Design Group, “Superconducting Supercollider Conceptual Design Report,” SSC-SR-2020, March 1986.
3. J. M. Peterson, “Choice of the Accelerating Frequency for the  $90^\circ$  Lattice and Related Parameters in the Injection Chain,” SSC-N-333, May 1987.
4. L. Schachinger and R. Talman, “TEAPOT: A Thin-Element Accelerator Program for Optics and Tracking,” *Particle Accelerators* **22**, p. 35 (1987).
5. M. A. Furman, “Effect of the Space-Charge Force on Tracking at Low Energy,” SSC-115, March 1987; “Practical Approximations for the Electric Field of Elliptical Beams,” SSC-N-312, April 1987.
6. M. A. Furman and J. M. Peterson, “Linear Space-Charge Tune Shifts for the SSC and its Injectors,” SSC-N-403, November 1987.